

Dome and Mirror Seeing Estimates for the Thirty Meter Telescope

John S. Pazder^a, Konstantinos Vogiatzis^b, and George Z. Angeli^b,

^aNational Research Council Canada, Herzberg Institute of Astrophysics

^bThirty Meter Telescope Observatory

Mirror and dome seeing are critical effects influencing the optical performance of ground based telescopes. The Thirty Meter Telescope project has been utilizing a combination of optical simulations and Computational Fluid Dynamics to model the dome and mirror seeing. A set of optical modeling tools has been developed in MATLAB to post-process high spatial resolution thermal CFD results and calculate image degradation due to dome seeing and mirror seeing. The same tools can provide the distribution of seeing contribution along optical path in order to recognize potential problems and guide the observatory design. The method, including limiting assumptions for the optical modeling tools are discussed.

Keywords: Thirty Meter Telescope, TMT, mirror seeing, dome seeing, thermal seeing

1. INTRODUCTION

This paper summarizes the current efforts of estimating the dome and mirror seeing effects for the Thirty Meter Telescope (TMT). This work is a continuation of ongoing mirror and dome seeing studies done at TMT^{1, 2}. This study has extended the previous work at TMT of estimating the three-dimensional C_n^2 field to computing the optical path difference (OPD) from the variations in air index variations for a wavefront traveling through the full telescope optical path.

This work is based on Computational Fluid Dynamics (CFD) modeling to compute the temperatures in and around the dome. The details of the CFD modeling are reported in a paper by Vogiatzis³ published in these proceedings. This paper is primarily concerned with the calculation of the seeing from the results of the CFD data, and the reader is urged to consult Vogiatzis's paper for details of the CFD modeling.

In our work we have defined 'mirror seeing' as the degradation of telescope image quality due to variations in the index of refraction of the air within 10cm of the primary mirror surface. 'Dome seeing' is defined as the degradation of telescope image quality due to variations in the index of refraction of the air caused by the dome, excluding the primary mirror seeing. Mirror seeing at the secondary and tertiary mirrors are currently not separated from the dome seeing. Simplified heat loads for these mirrors are included in the CFD model to account for seeing at these mirrors in a limited way. The Dome seeing is not limited to seeing effects within the dome, but include seeing effects outside the dome aperture caused by the dome itself. In the CFD modeling ground layer effects are included in the model to compute the correct temperature and flow characteristics over the dome. Dome seeing is separated from ground layer seeing by truncating the computation at the point the dome effects cease to be significant.

2. CALCULATION OF DOME SEEING

The goal of our dome seeing modeling is to provide an accurate model of the degradation of the telescope image quality due to variations in the index of refraction of the air caused by the dome. In line with this goal, a number of simplifying assumptions have been made to reduce this problem from a volumetric ray tracing to one of computing the OPD using a series of 'phase screen' through the optical path.

We assume we can compute the diffraction image by summing the OPD error through the system, applying this to the exit pupil, and propagating from the exit pupil to the image using the Fourier transform of the exit pupil ignoring the propagation effects within the system. This requires a number of conditions to be met; the reader is referred to Shannon⁴

for details of all the necessary conditions. Because the TMT is a typical imaging system with a reasonable $F/\#$, the telescope, without seeing, meets the necessary conditions to compute the diffraction image by this method.

It is worth while to examine the seeing to see it also satisfies these conditions. The requirement that the dome seeing on TMT be a small fraction of an arc second means the seeing phase errors have small slope errors, of the magnitude of the angular seeing size. This requirement on the dome seeing tells us the extended sine condition is satisfied and puts a limit on the required sampling at the pupil. To correctly sample the wavefront we need the phase error across each grid point to be less than a quarter wave. Taking a maximum slope error of half an arc second (a value much larger than we expect) at a wavelength of one micron, the necessary entrance pupil sampling pitch is 0.4m or less. We have chosen a conservative entrance pupil sampling pitch of 0.2m. It is worth while to think further about why dome and mirror seeing are a problem in telescopes, and not for smaller optical instruments. This is because of the large optical paths involved in the telescopes and the large thermal mass of the large mirrors. In both cases, these phase errors accumulate far from the focus compared to the wavelength so we can ignore near field diffraction effects and ‘full propagation’ of the wavefront is unnecessary.

We also assume the lateral aberrations introduced by the seeing are smaller than the lateral sampling of the wavefront along the path. This assumption allows us to ignore the ‘ray deviation’ due to seeing along the path, and simply sum the OPD along ‘ray’ paths given by the telescope optics for an un-aberrated telescope. Given the requirement that the dome seeing on TMT be a small fraction of an arc second, the maximum ray deviation from the pupil to the image is a fraction of a millimeter. We stop our dome seeing calculation at the start of the instrument area, 5m from the finial focus. Here the grid pitch is 2mm, much larger than the maximum ray deviation.

The small magnitude of the dome and mirror seeing and distance from the focus for the seeing effects means the necessary conditions are met. We can safely sum the OPD error through the system, apply this to the exit pupil, and propagate from the exit pupil to the image using the Fourier transform.

We also ignore the static aberrations of the optical system due to the optical design residuals, and assume the dome seeing is reasonably invariant to the exact shape of the optics. This invariance allows us to use a spheroid shape for the primary and a planar shape for the secondary in the CFD model. We also ignore the primary mirror segmentation and approximate the telescope pupil as a circular aperture with a circular central obstruction. We can now trace approximate ‘rays’ to a spherical primary, to the planar secondary and onward, and compute the OPD introduced by the variations in the index of refraction of the air along these paths for the dome seeing.

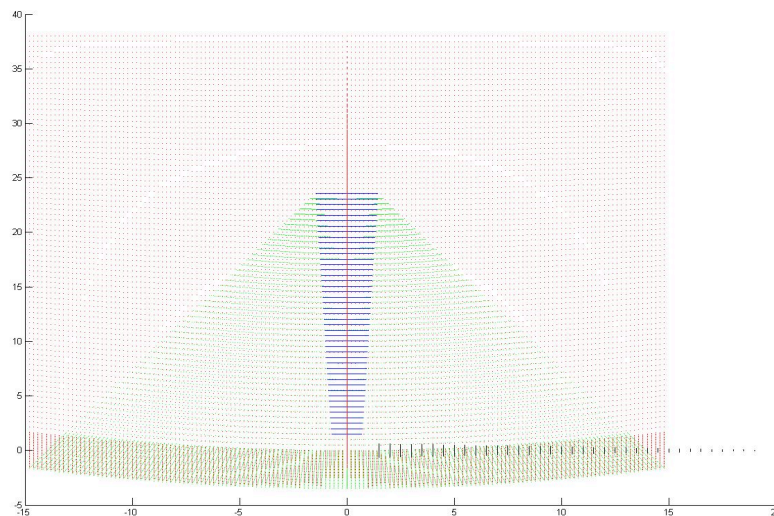


Figure 1: Data Screen geometry

We understand that at times a large portion of the seeing occurs close to the primary mirror and to accurately model the seeing we want to be sampling close to this surface. To accomplish this, the CFD node geometry data is refit to a series of regular ‘screens’ which are a progression of spheres. These ‘screens’ are scaled in width to follow the optical beam or “ray paths” through the system. With this scaling to follow the beam through the system each grid point on the ‘screens’ follows the path a ray would follow in the system. The geometry of these ‘screens’ is shown in Figure 1. These screens now represent the temperature as predicted by the CFD model, but fitted to regular 2d screens scaled to follow the ray paths.

The TMT telescope is a three mirror system, two conic mirrors (the primary and secondary) configured as a Ritchey Chrétien telescope with a plano tertiary steering mirror to guide the light to the Nasmyth instrument platforms. As can be seen in Figure 1, we have stopped our screens 1.5m before and started them 1.5m after the tertiary mirror (m3) before continuing to follow the light to the instrument platform on the right. This was done to avoid the complexity of fitting the screens to the angled tertiary. The seeing near the tertiary is currently being ignored in our modeling. In addition, to capture the increased turbulence near the primary mirror, we have increased the sampling along the optical path to 0.1 m steps from the 0.5m steps in the rest of the path. Screens are shown in Figure 1 up to the focus for clarity of the figure, in the calculation we stop 5m from the focus, at the start of the instrument area. The size of each screen is 149 x 149 across, equal to a sample pitch of 0.2m across the wavefront at the primary.

To compute the OPD, this temperature data needs to be converted to refractive index. The following equation is used⁵:

$$n_{air} = 1 + \frac{(n_{ref} - 1)P}{1 + 3.4785e^{-3} * (T - 15)}$$

where

$$n_{ref} = 1 + 1.0e^{-8} * \left[6432.8 + \frac{2949810\lambda^2}{146\lambda^2 - 1} + \frac{25540\lambda^2}{41\lambda^2 - 1} \right]$$

and T is in Celsius, λ in microns and P in atmospheres. A uniform pressure of 0.7 atmospheres is assumed for all calculations.

To convert this to OPD, we recall optical path length (OPL) is given by

$$OPL = \int ndL = \sum n_i d_i$$

We have N ‘screens’ of index of refraction along the optical path, we compute OPL_i as the optical path difference for screen i to screen (i+1). We take the index of refraction of this screen as the average of the index at screen i and screen (i+1). The distance d_i is the distance from the points in screen i to screen (i+1) so

$$OPL_i = \frac{(n_i + n_{i+1})}{2} \cdot \left| (\vec{P}_{i+1} - \vec{P}_i) \right| = n_{avg_i} \cdot d_i \quad (\text{calculated for each point on the screen, where P is the position vector of the respective point on the screen})$$

so

$$OPL = \sum OPL_i = \sum n_{avg_i} \cdot d_i$$

We want OPD, the change in OPL from a reference distance; we adopt as a reference distance the OPL for the system at a uniform index equal to mean of the index of refraction in the entire optical path:

$$OPD = OPL - OPL(ref)$$

$$OPD = \sum n_{avg_i} \cdot d_i - \sum n_{mean} \cdot d_i$$

$$OPD = \sum (n_{avg_i} - n_{mean}) \cdot d_i$$

and we define dn_i as the change in index from the mean index so:

$$OPD_i = dn_i \cdot d_i \quad \text{where} \quad dn_i = n_{avg_i} - n_{mean}$$

and

$$OPD = \sum OPD_i$$

The CFD data is a time series, representing the flow over time for the telescope. The above method has been implemented in Matlab to allow both the OPD along the optical path, as well as the OPD over the time series to be computed.

As an example of the dome seeing analysis tool output the results for the telescope pointing at 32 degrees from zenith and 0 degrees azimuth (azimuth is with respect to the wind so 0 degrees azimuth corresponds to the telescope mirror facing into the wind) for both the enclosure vents open and closed are given in Figures 2 to 5. One useful output from the tool to help visualize the dome seeing performance is the movie output. Figure 2 shows the first frame of the movie output for the case with the vents open. Both the pupil OPD and point spread function are displayed in the output with a number of other performance metrics.

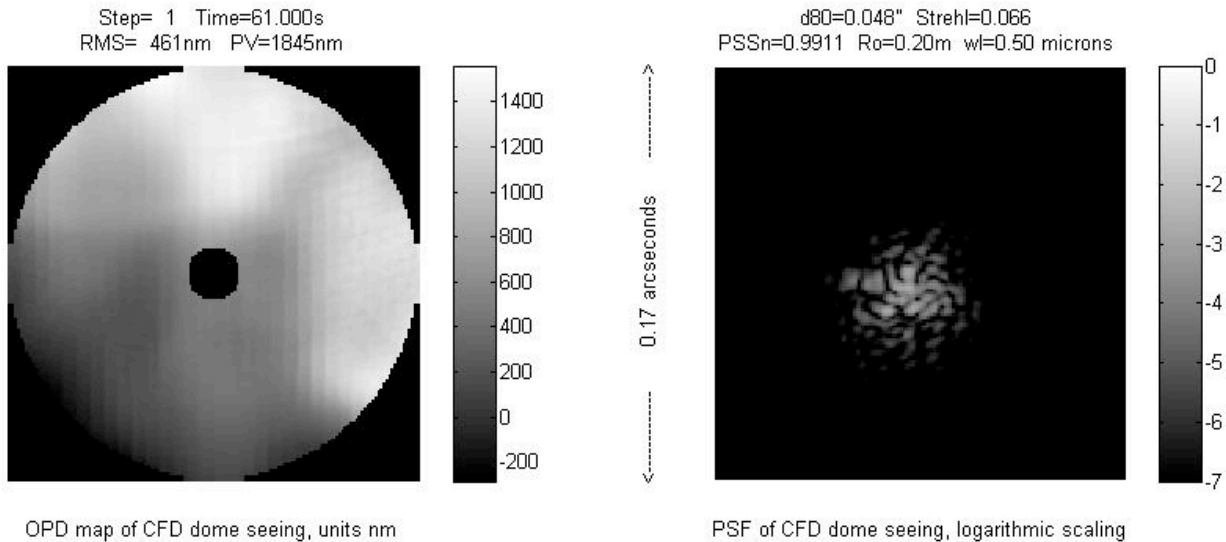


Figure 2: OPD and PSF for the telescope at zenith angle 32, azimuth 0 with vents open

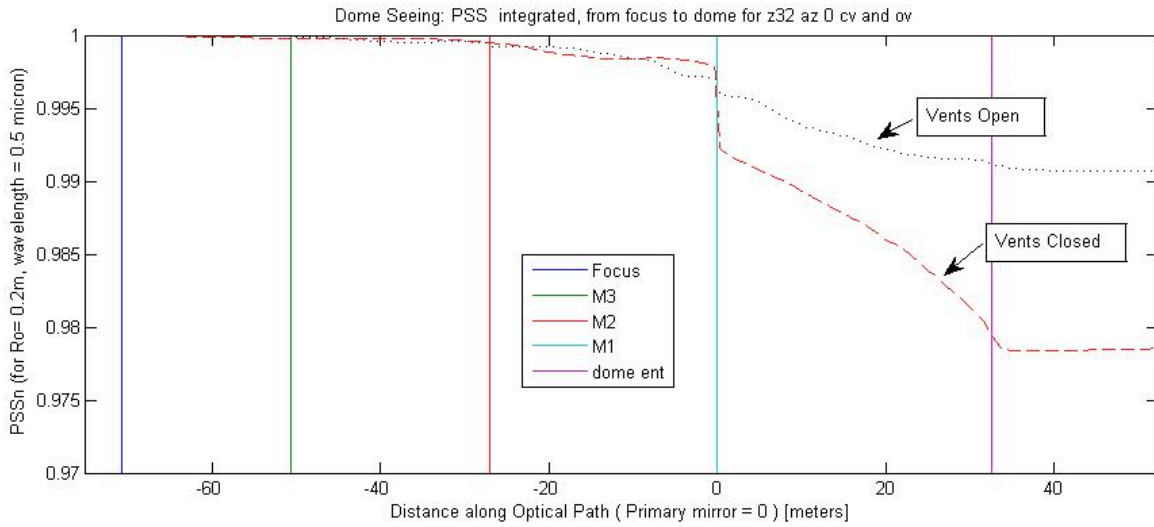


Figure 3: Dome Seeing integrated from focus to dome entrance and out for telescope at zenith angle 32, azimuth 0 for open and closed vents

In Figure 3 the seeing integrated along the optical path from the focus to the tertiary, to the secondary, to the primary, and out the dome is shown. The metric plotted is the Point Source Sensitivity normalized to the atmospheric seeing (PSSn). This metric is representative of the relative integration time of a background limited point source observation normalized to the atmospheric seeing. A full discussion of this metric is given by Seo⁶.

It can be seen in the plot that the optical path from the focus to the primary mirror (from -60m to 0m) contributes in a small way to the seeing. At the primary mirror for the vents open case there is a small amount of mirror seeing which occurs outside of the 10 cm distance from the primary mirror which we have used to segregate dome seeing from mirror seeing. For the case with the vents closed, there is considerably more primary mirror seeing due to the lack of mirror flushing. Seeing from the primary to the dome entrance is also more for the vents closed case. Outside the dome we see very little additional drop in seeing indicating we have a good flow around the enclosure. The external wind for the vents open case was 3m/s while for the vents closed case it was 10m/s, so the lower performance of the vents closed case with worse performance is also indicative of the higher external wind speeds. Figure 4 shows the CFD temperature profile of the vents open and closed cases for the first time step in the run.

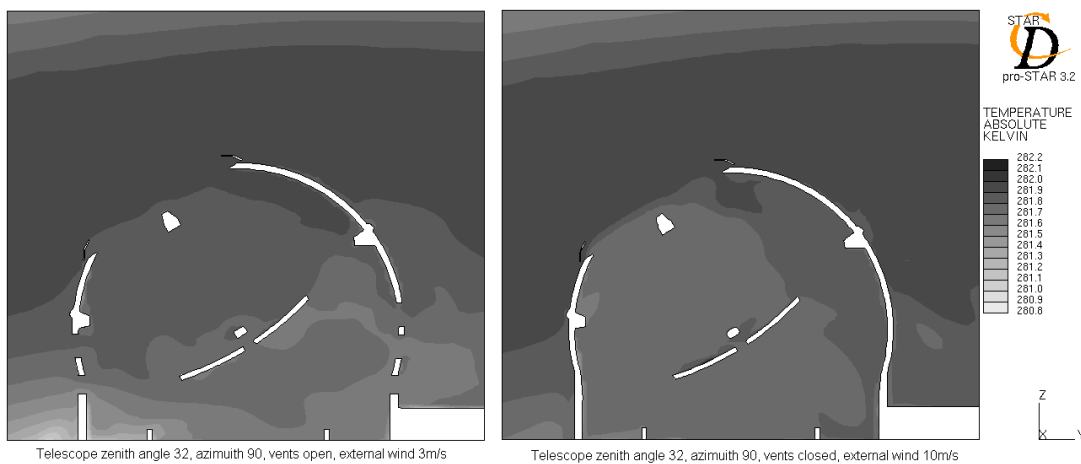


Figure 4 : CFD temperature profile for the telescope at zenith angle 32, azimuth 0 with vents open and closed

An important use of the dome seeing results is in the Monte Carlo simulation framework⁷. The results are incorporated in a dome seeing estimation function which interpolates a matrix of PSSn results parameterized as a function of telescope zenith angle, azimuth angle, and atmospheric Ro. Figure 5 shows PSSn as a function of Ro for the dome configurations we have discussed so far. These are two vectors of the PSSn results matrix. The results matrix contains several telescope orientations and configurations for accurate interpolation of dome seeing in the simulation framework.

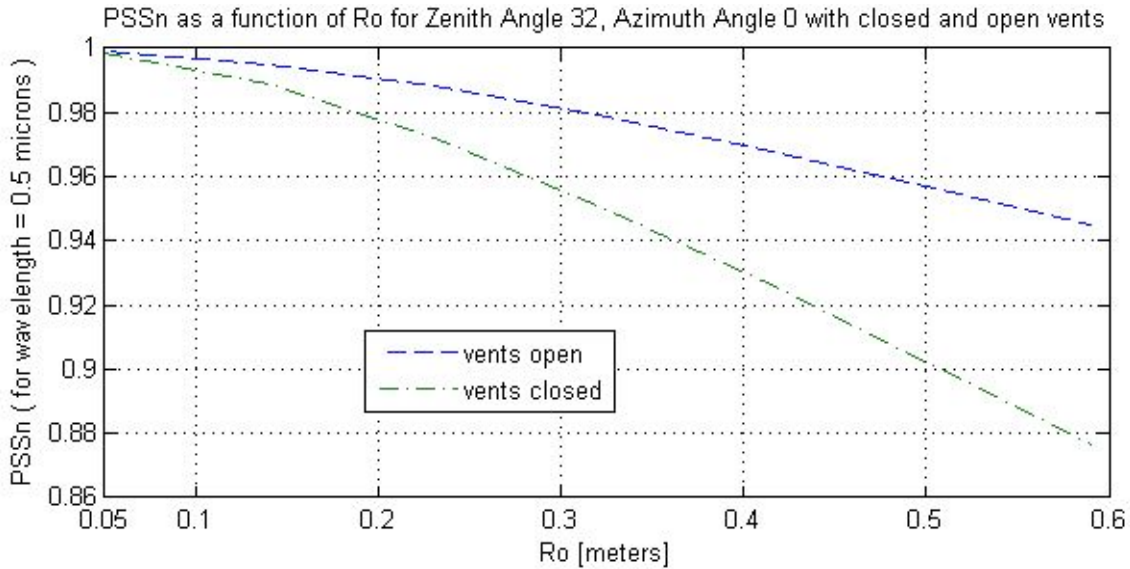


Figure 5: PSSn as a function of Ro for telescope at zenith angle 32, azimuth 0, for vents open and closed

3. PRIMARY MIRROR SEEING

The primary mirror seeing (defined as the seeing within 10cm of the primary mirror) has been separated from the dome seeing in our modeling. This separation has been done because the mirror seeing is strongly dependent on the history of the thermal environment due to the heat capacity of the mirror resulting in a thermal “memory”. This thermal memory adds complexity to the Monte Carlo framework where the mirror seeing results are needed to model the overall performance of TMT. A simple look up table can not be used. An unsteady solution to the heat transfer needs to be done within the Monte Carlo framework. This imposes a specific requirement on the mirror seeing in that we must be able to solve the heat transfer and compute the mirror seeing in a few milliseconds in order for the Monte Carlo framework to run within a reasonable time.

The primary mirror thermal model is discussed in detail by Vogiatzis⁷. This model includes rear heat loads from actuators and preamps on the back of the segments⁸ and a heat transfer at the front based on radiation and convective cooling. To sample the heat loads on the rear of the primary mirror, a 120x120 grid with 0.25m sampling across the primary mirror is used for the temperature map of the temperature differences between the mirror surface and the mirror seeing boundary (10cm above the primary).

The index of refraction of the air is computed from the temperature map using the same equation as in the dome seeing case. We assume a simple linear index variation from the mirror seeing to the boundary so the average index of the boundary is half of the temperature differences between the mirror surface and the mirror seeing boundary, thus with the double pass of the beam to and from the mirror the factor of one half disappears and the OPD in meters is $0.1 \cdot dn$.

To calculate the PSSn from the mirror seeing OPD map we need the OPD sampling to be fine enough to capture atmospheric seeing. With our 0.25m grid increment, we have clearly under sampled the OPD. In the Dome seeing case, the OPD was interpolated before the PSSn calculation to capture the atmospheric seeing. In the mirror seeing case, we would like to avoid interpolating the OPD as such a PSSn calculation would be too slow for the Monte Carlo framework.

The PSSn we are calculating is given by:

$$PSSn = \frac{\int_{-\infty}^{\infty} \int_{-\infty}^{\infty} |MTF_{aberrated} * MTF_{atm}|^2 dA}{\int_{-\infty}^{\infty} \int_{-\infty}^{\infty} |MTF_{perfect} * MTF_{atm}|^2 dA} = \frac{\Delta \sum (MTF_{aberrated} MTF_{atm})^2}{\Delta \sum (MTF_{perfect} MTF_{atm})^2}$$

The computation of the mirror seeing MTF for the PSSn integral requires two Fourier transforms of the OPD, so we wish to transform as small as a grid as possible to compute the MTF fast. To remove the need to interpolate the OPD and do big Fourier transforms we draw on the Nyquist sampling theorem. This states if we have critically sampled the data, we have all the information and we can compute the intermediate points in the data with Fourier interpolation⁹. Now the maximum sampling frequency needed for the OPD is the mirror seeing critical frequency.

In practice, Fourier interpolation is too slow, and since the MTF is windowed by the atmospheric MTF we need only interpolate over the area where the convolution of the mirror seeing with the atmosphere contributes meaningfully to the PSSn integral. To determine the size of this window we compute the denominator of the PSSn and find the radius where the error in MTF is insignificant assuming $MTF_{perfect} = 1$ (this is equivalent to an infinite aperture). Thus we wish to evaluate:

$$error = 1 - \frac{\int_0^R MTF_{atm}^2 d\Omega}{\int_0^{\infty} MTF_{atm}^2 d\Omega}$$

For an error of < 0.001 we need to integrate to $\lambda f/Ro = 5.07$, for < 0.0001 we need to integrate to $\lambda f/Ro = 5.98$. So to be safe, we take the latter, and we extract the area in mirror seeing MTF where $f < 5.98 Ro/\lambda$ and interpolate this area to get the sampling in MTF we need.

The amount we need to interpolate the mirror seeing MTF can be reduced by sub-integrating the atmospheric MTF before we the piecewise integrate the PSSn. Without doing this we would have interpolate the atmospheric MTF at a rate sufficient to sample the curvature of the atmospheric MTF to eliminate the trapezoidal integration error in the PSSn computation. An example of where the atmospheric MTF is piecewise integrated at a rate of 10x the mirror seeing is:

$$PSSn = \frac{\sum_{i=1,11,21...}^n (MTF(i)_{aberrated})^2 \sum_{j=i}^{i+9} MTF_{atm}^2}{\sum_{i=1,11,21...}^n (MTF(i)_{perfect})^2 \sum_{j=i}^{i+9} MTF_{atm}^2}$$

Because we are able to pre-compute the sub-integration or decimation of the atmospheric MTF our computation time of the PSSn in the Monte Carlo framework is significantly reduced. Empirically, it was determined for an atmospheric MTF sub-integration of 5x the mirror seeing MTF that ~ 1.8 samples across Ro/λ is sufficient sampling of the mirror seeing MTF. So the required interpolate of the mirror seeing MTF is ~ 21 samples across the extracted area. Here we have essentially applied the Nyquist sampling theorem a second time.

In the mirror seeing estimation tool, as much as possible is pre-computed before the Monte Carlo run. The mirror seeing PSSn is a function of R_o ; to allow further pre-computation the R_o value is rounded to the nearest cm for the PSSn calculation. The above methods improves the PSSn calculation efficiency so we may compute an accurate PSSn using only 120x120 sampling of the OPD and perform the PSSn calculation of mirror seeing in 10ms to 15ms on our workstation.

The PSSn for a mirror seeing over a typical night in the Monte Carlo network is shown in Figure 6 and an OPD map at 25% of this night is shown in Figure 7.

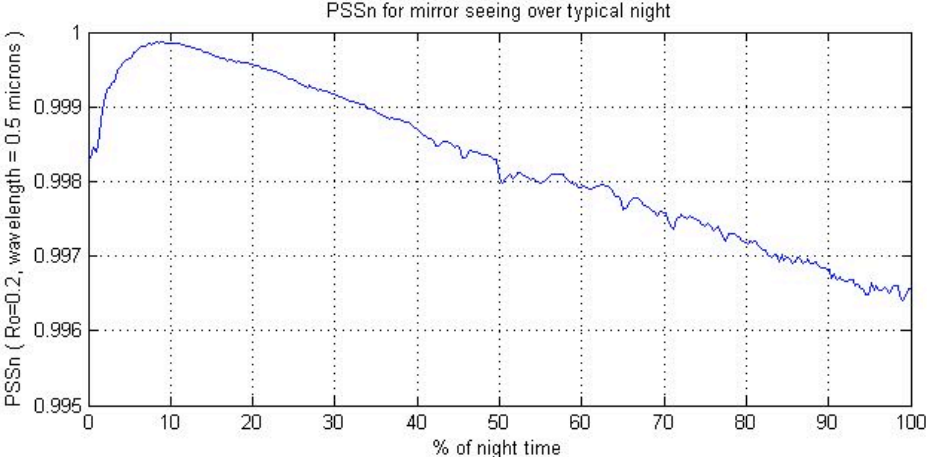


Figure 6: PSSn for mirror seeing over typical night

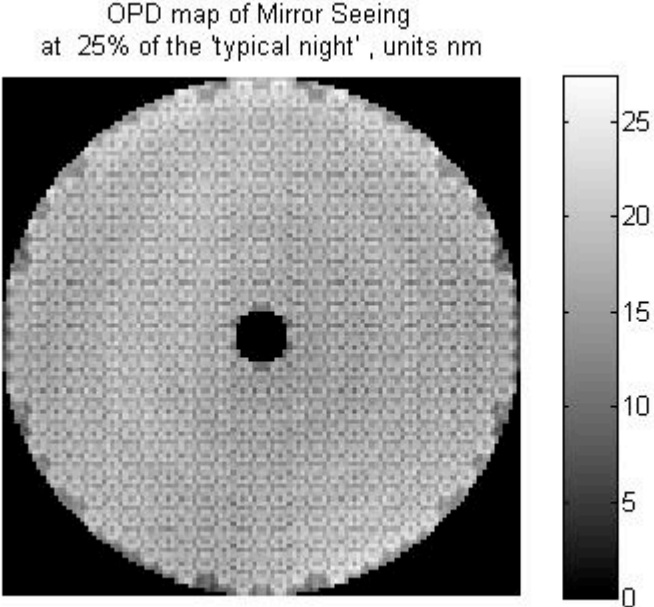


Figure 7: Mirror Seeing OPD map at 25% of the 'typical night'

4. CONCLUSIONS

The Matlab tool developed for modeling dome seeing model provides a new method to compute the dome seeing from CFD results. In addition to providing results for the TMT Monte Carlo simulation framework, the tool can be used to aid in our understanding of the dome seeing by presenting the data in time series, or seeing as a function of altitude.

The separation of mirror seeing from dome seeing in the Monte Carlo simulation framework was necessitated due to the problem of thermal history for the primary mirror. This resulted in the need to solve a numerical analysis problem of computing the PSSn of the primary mirror seeing in a very short time for the Monte Carlo simulation framework. The method derived is able to perform the calculation within the required time.

ACKNOWLEDGMENTS

The authors gratefully acknowledge the support of the TMT partner institutions. They are the Association of Canadian Universities for Research in Astronomy (ACURA), the California Institute of Technology and the University of California. This work was supported as well by the Gordon and Betty Moore Foundation, the Canada Foundation for Innovation, the Ontario Ministry of Research and Innovation, the National Research Council of Canada, the Natural Sciences and Engineering Research Council of Canada, the British Columbia Knowledge Development Fund, the Association of Universities for Research in Astronomy (AURA) and the U.S. National Science Foundation.

REFERENCES

- [1] Vogiatzis, K. and Upton, R., "TMT Studies on Thermal Seeing Modeling: Mirror and Dome Seeing Model Validation", Proc. SPIE 6271, 627115 (2006).
- [2] Vogiatzis, K., and Angeli, G., "Strategies for Estimating Mirror and Dome Seeing for TMT", Proc. SPIE 6271, 62710O (2007).
- [3] Vogiatzis, K., "Advances in AeroThermal Modeling for TMT", Proc. SPIE 7017 (2008)
- [4] Shannon, R. R., [The Art and Science of Optical Design], Cambridge University Press, (1997).
- [5] Kohlrausch, F., [Praktische Physik, Vol 1], Teubner, Stuttgart, p 408, (1968).
- [6] Seo, B-J., et.al., "Analysis of Normalized Point Source Sensitivity as a performance metric for the Thirty Meter Telescope", Proc. SPIE 7017 (2008)
- [7] Vogiatzis, K., and Angeli, G., "Monte Carlo Simulation Framework for TMT", Proc. SPIE 7017 (2008)
- [8] Cho, M., et.al., "Thermal performance prediction of the TMT optics", Proc. SPIE 7017 (2008)
- [9] Bracewell, R., [The Fourier Transform and It's Application], McGraw-Hill, (1965).